Supplementary information

Probing inhomogeneous diffusion in the microenvironments of phase-separated polymers under confinement

Marjan Shayegan[1], Radin Tahvildari[1], Kimberly Metera[1], Lydia Kisley[2], Stephen W. Michnick[3], Sabrina R. Leslie[1]

[1]Department of Physics, McGill University; [2]Department of Physics, Case Western Reserve University, Cleveland, Ohio, United States; [3]Département de Biochimie, Université de Montreal

S1. Materials and Experimental Methods

Dextran-PEG system: Fluorescein isothiocynate (FITC)-dextran (molecular weight 400–500 kDa) and PEG (average molecular weight 8 kDa) were purchased from Sigma-Aldrich and used without further purification. Solutions of 2 wt% dextran in distilled water were first loaded into the flow cells and confined in pits. Then PEG (12 wt% in distilled water) was loaded through fabricated microchannels in the device to initiate phase separation. To perform passive microrheology, 20-nm carboxylate-modified microspheres with crimson fluorescence (625/645) were purchased from Thermo Fisher Scientific and passivated with dextran by incubating them in 24 wt% dextran overnight. The dextran present in the particle solution (for non-specific passivation) was considered for the final concentration of dextran solution for the experiment. The bead concentration was chosen to give an average of one bead per condensate for 3 μm diameter condensates and 3-5 beads for larger condensates.

Dhh1-poly(U) system: Dhh1- mCherry was kindly provided by Dr. K. Weis at ETH Zurich and condensates were formed using their protocols [1]. Dhh1 was first diluted in 50 μM in 1x ATPase buffer (30 mM HEPES-KOH pH 7.5, 100 mM NaCl, 2 mM MgCl$_2$). A reaction mixture was prepared with in vitro reconstitution buffer (75 mM KCl, 15 mM HEPES KOH pH 7.4, 2 mM MgCl$_2$), 15 mM EPES-KOH pH 6.6, 0.5 mg/ml BSA, 0.075 mg/ml Poly(U) (molecular weight 100 - 1000 kDa, purchased from Sigma-Aldrich), 1X RNAse inhibitors (purchased from Sigma-Aldrich), 5 mM ATP and 10 mM

MgCl$_2$. Finally, for confinement microscopy experiments, Dhh1 was added to the reaction mixture to get a protein concentration of 12 µM (See Supplementary Figure S4 for the effect of protein concentration on phase separation). To perform passive microrheology, 48-nm carboxylate-modified microspheres with dark red fluorescent (660/680) from Thermo Fisher Scientific were passivated with 10 mg/ml BSA for 1 hour. With our dual-color fluorescence imaging system, we verified that there is no accumulation of proteins on the surface of tracer particles. Hence, we ruled out the possibility of tracer-matrix interactions affecting movement of the tracer particle within the droplet. In addition, to confirm that proteins have not misfolded or aggregated during our experiment, we tested the reversibility of condensed droplets by flowing more reagents such as RNA (in the protein/RNA system) or PEG (in the dextran/PEG system), and we did see dissolution of droplets.

Confinement microscopy experiments:

The CLiC (Convex Lens-induced Confinement) instrument used in these experiments is described in Ref. [2]. The flow cell is made of two 25×25-mm^2 glass substrates separated by a 10-µm thick double-sided adhesive (Nitto Denko, Product No. 5601). The bottom layer of the flow cell, made of a 200±10-µm thick cover glass (Ted Pella, Product No. 260452), contains a micro-well array with the diameter range of 3 to 50 µm and 450±20 nm in depth. The top layer, made of 150±20-µm thick standard microscope cover slips (VWR, Product No. CA48366-089-1), consists of 10 µm diameter posts arrayed to create a stable confinement across the imaging region and provide enough space to exchange reagents with the confined solutions. There are also two holes drilled diagonally on two sides of the top glass layer for sample introduction. Both the top and bottom layers are first patterned by photolithography with their corresponding designs then dry-etched by reactive ion etching (RIE) to obtain the engraved features. (Further information about the flow cell fabrication can be found in Ref. [3]). The assembled flow cell is then sealed in a custom microfluidic chuck [2]. Using a convex lens mounted on a piezoelectric actuator, the top coverslip was deformed and lowered down into contact with the bottom coverslip, as described in Ref. [2]

Imaging procedure: For imaging, a Nikon CFI Apo TIRF 100× oil-immersion objective lens with NA 1.49 was used. The flow cell and chuck were placed on a sample plate and the objective brought to the focal height, to focus on the wells. As the top surface was brought into contact with the bottom surface, the center of the confined region was aligned to the well array. For particle tracking, videos were acquired with 1000 frames at 50 ms exposure time and 74 ms intervals between frames.

S2. Particle Position Analysis

Movies were recorded of the motions of the embedded beads within condensates formed in arrays of wells; the videos were manually cropped into multiple videos, each including a single bead. In rare cases beads became immobilized on the surface of the condensate, rather than inside, and were removed from the analysis. These particles were identified as the ones with less than 10^{-5} μm^2 over all time delays (essentially plateau MSD). For each frame in a bead video, a custom particle detection routine written in MATLAB was used. The program first applies a two-dimensional Gaussian filter on each image (each frame of the spatially cropped video) with a smoothing kernel with standard deviation of two pixels (pixel size is 160 nm). Then, a two-dimensional Gaussian function is fitted to the constructed matrix of the filtered intensity values in that image. The maximum point of this fitted surface gives the position of the bead in this frame with sub-pixel resolution. This process is repeated for each frame in order to track the position of the bead over time. Time-averaged mean squared displacements (MSD) of embedded particles were calculated versus lag time. Finally, static error of the bead's displacement was subtracted by analyzing displacement of a stuck bead on the bottom coverslip. Figure S1 shows an example of MSD values obtained by averaging MSD values over 10 different beads diffusing in a solution of 2 wt% dextran confined in wells of 3 μm diameter. At short decay times (less than 1 second), MSD values increase approximately linearly with time, an indication of Brownian motion within the solution. However, at long enough times (greater than ~2 seconds), the MSD curve is saturated as a function of time because the beads were confined to wells of finite area.
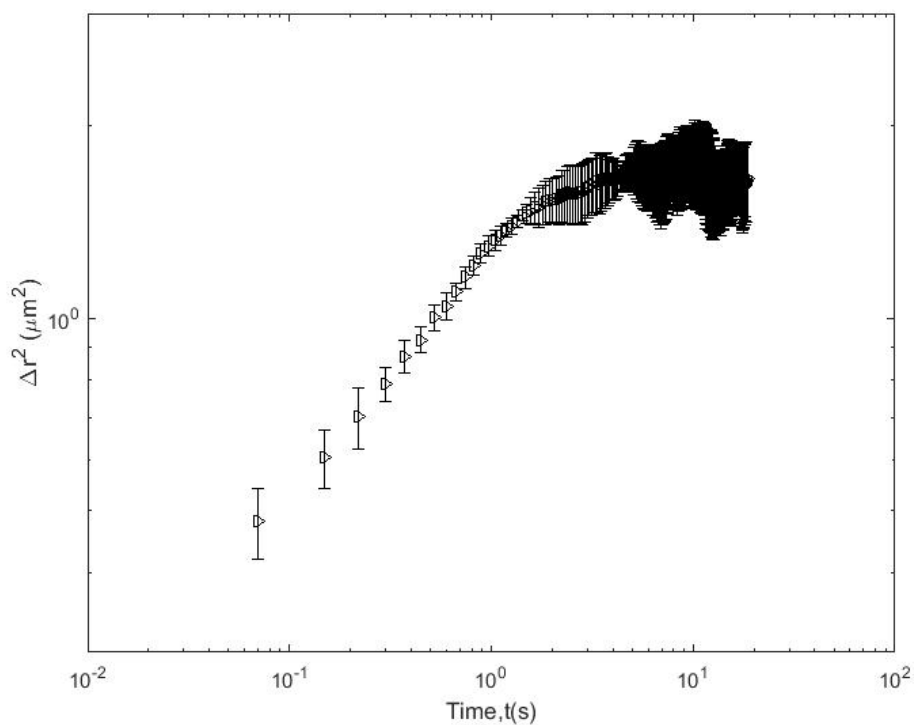
Figure S1. Homogenous, confined Brownian diffusion is observed within a solution of pure dextran. Time- and ensemble averaged mean squared displacement of 20 nm probe particles in 2 wt% dextran solution confined in wells of 3 μm diameter. At short time scales, i.e. less than 1 s, normal diffusion is observed, however, at long time scales a particle's motion is confined by the well's walls. Data points in this plot are an average of 10 particle trajectories and the error bars show standard error of the mean.

S3. Correlation Analysis

Correlation analysis was based on a previously reported technique [4]. All correlation analysis was performed in MATLAB. The collected data were converted to a 3D image stack compatible with MATLAB. At each individual pixel over time, second-order correlation was performed with the built-in MATLAB function "xcorr". The resulting autocorrelation data is $G_2(r,\tau)$, where r is the pixel and τ is the time lag. The data were normalized by the maximum value at a time lag equal to one frame. $G_2(r,\tau)$ was then log binned versus time to avoid noise artifacts in the analysis.

For each individual data set of beads within the phase separated condensates, the pixel with the maximum value of $G_2(r,\tau)$ at the time lag of one frame was used and is defined as r_{max}. The resulting $G_2(r_{max},\tau)$ for each trial based on the condensate size and composition was averaged over τ. The average curve was then fit to a two-component diffusion equation where one component was anomalous:

$$G_2(r, \tau) = A_a \frac{1}{1+\tau/\tau_{Da}{}^\alpha} + A_b \frac{1}{1+\tau/\tau_{Db}} + c \qquad \text{(Eq. S1)}$$

In Equation S1, α is the anomalous diffusion factor which deviates from 1 when diffusion is no longer Brownian, A_a and A_b represent the amplitude of the anomalous and Brownian components, τ_{Da} and τ_{Db} are the characteristic anomalous and Brownian diffusion times across the pixel for which the autocorrelation was performed, and c is a constant offset. The first data point was ignored during fitting, as fluctuations on the time scale of one frame were shown to be due to camera noise and crosstalk in control measurements. The fitting always resulted in $\tau_{Da} > \tau_{Db}$.

Table S1. Correlation analysis fitting results for Figures 3c and 4c

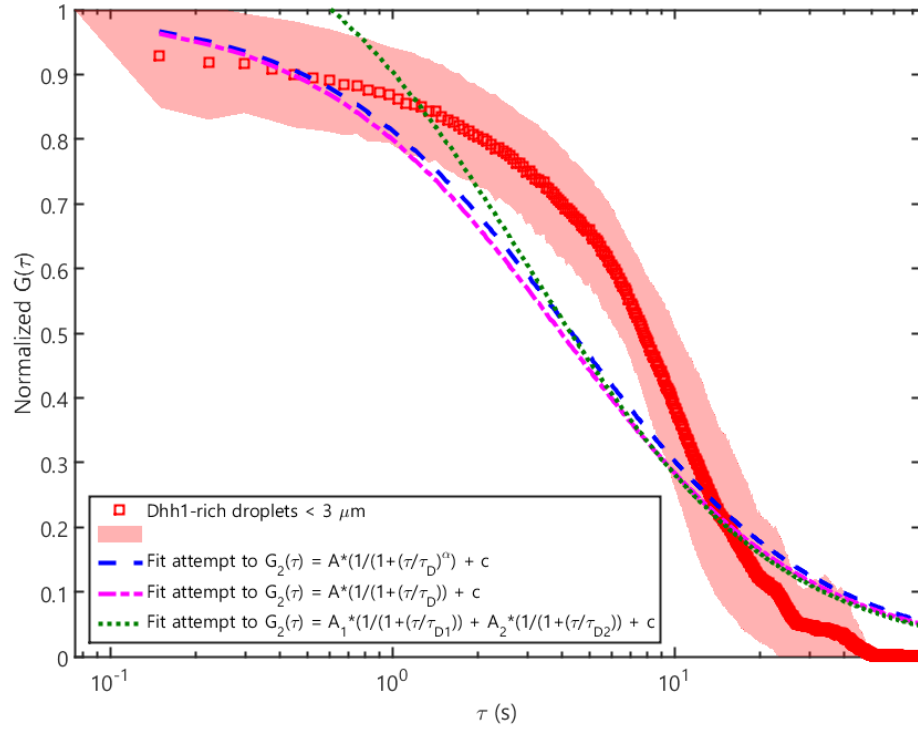| Sample	Size (μm)	α	A_a (%)	τ_a (s)	A_b (%)	τ_b (s)
Dextran-rich	≤ 3	2.9 ± 0.3	23 ± 1	32 ± 1	76 ± 2	3.0 ± 0.3
Dextran-rich	> 3	1.45 ± 0.09	80 ± 10	7.5 ± 0.8	25 ± 8	0.5 ± 2
Dhh1-rich	≤ 3	2.48 ± 0.04	75 ± 2	9.91 ± 0.09	26 ± 2	0.6 ± 0.2
Dhh1-rich	> 3	2.4 ± 0.1	69 ± 2	9.6 ± 0.1	30 ± 2	1.1 ± 0.2

Figure S2. Alternative fittings of simpler diffusion equations fail to adequately fit the data. Example attempts to fit the Dhh1-rich condensates ≤ 3 μm in size with one-component anomalous (blue), one-component Brownian (pink), and two-component Brownian (green) models. Similar poor fits with non-random residuals were observed for the other Dhh1-rich and dextran-rich data.
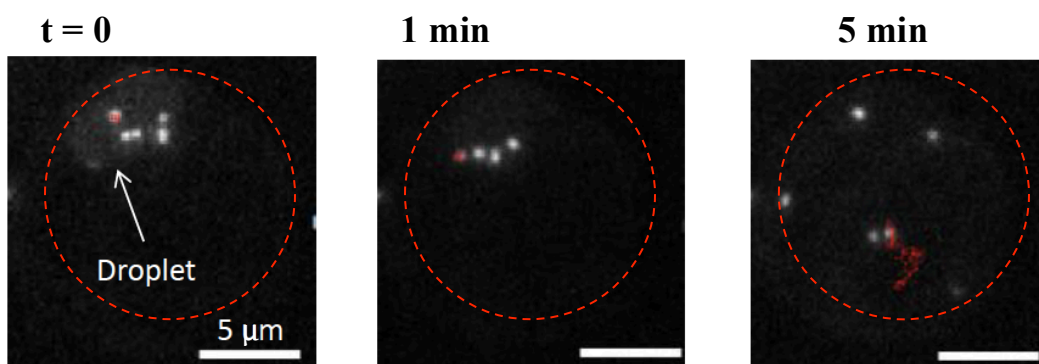
Figure S3. Addition of protein NOT1 disassembles pre-formed Dhh1 condensates. Embedded particles (bright dots) are shown with their time trajectories (over 5 seconds) in red for different time points during disassembly. Embedded beads inside condensates start to diffuse faster as the condensate is disassembling. Root-mean-squared displacement of these embedded particles are approximately 100 nm, 300 nm, and 1.5 μm over 5 seconds for t=0, 1 min, and 5 min, respectively. Dotted circles show the location of the wells.
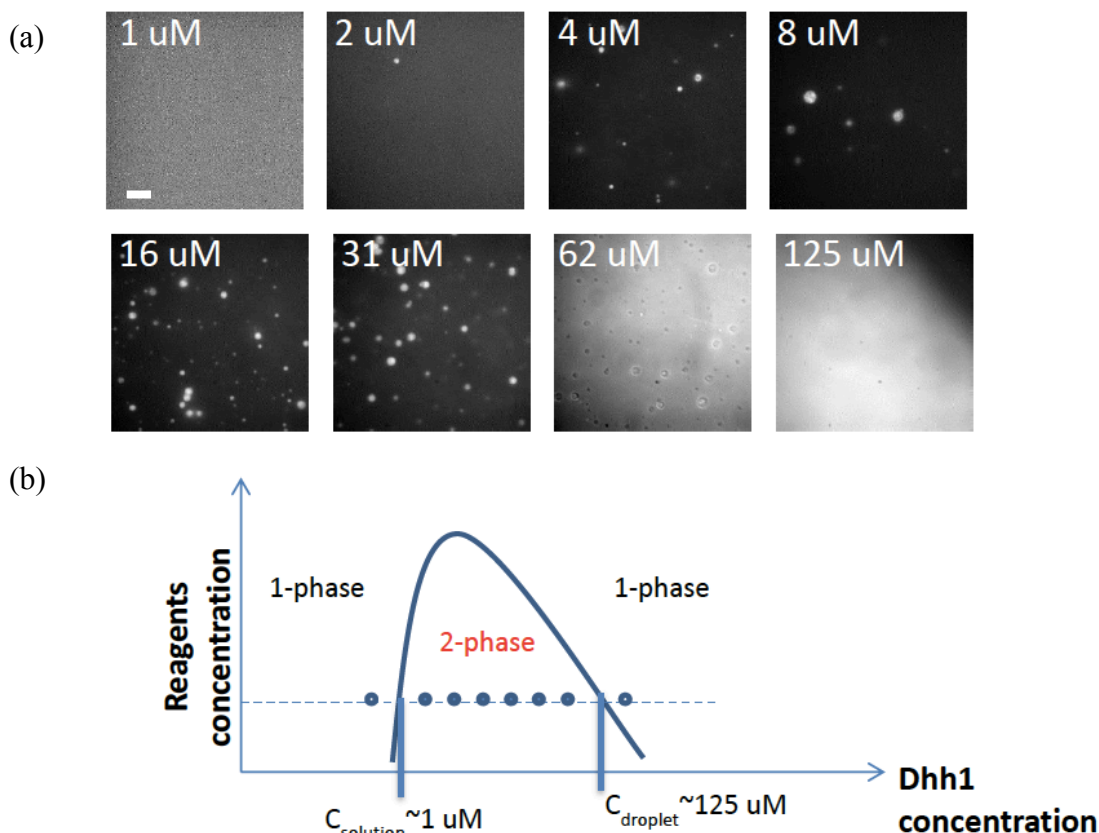
Figure S4. Estimation of protein concentration inside Dhh1-poly(U) condensates by imaging condensate formation on an open surface (*i.e.* without confinement): (a) Formation of Dhh1-condensates increases by increasing protein concentration up to ~31 μM Dhh1. The scale bar is 10 μm. (b) Schematic showing a typical binodal with increasing protein Dhh1 concentration. For a given reagent (all, except protein) concentration, the left arm of the binodal defines protein concentration outside the condensate (i.e. solution concentration), while the right arm of the binodal defines protein concentration inside the condensate. According to the fluorescence images in (a), condensation only starts to be happening at protein concentrations greater than 1 μM and less than 125 μM. Therefore, at the particular reagent concentrations used here, left and right arms of the bimodal are estimated to be at 1 and 125 μM.

References:

1. Mugler, C. F.; Hondele, M.; Heinrich, S.; Sachdev, R.; Vallotton, P.; Koek, A. Y.; Chan, L. Y.; Weis, K. ATPase activity of the DEAD-box protein Dhh1 controls processing body formation. *Elife* **2016**, 5, e18746.

2. Berard, D. J.; Shayegan, M.; Michaud, F.; Henkin, G.; Scott, S.; Leslie, S. R. Formatting and ligating biopolymers using adjustable nanoconfinement. *Appl. Phys. Lett.* **2016**, 109, 033702.

3. Henkin, G.; Berard, D.; Stabile, F.; Shayegan, M.; Leith J. S.; Leslie, S. R. Manipulating and Visualizing Molecular Interactions in Customized Nanoscale Spaces. *Anal. Chem.* **2016**, 88, 11100–11107.

4. Kisley, L.; Brunetti, R.; Tauzin, L. J.; Shuang, B.; Yi, X.; Kirkeminde, A. W.; Higgins, D. A.; Weiss, S.; Landes, C. F. Characterization of Porous Materials by Fluorescence Correlation Spectroscopy Super-resolution Optical Fluctuation Imaging. *ACS Nano* **2015**, 9, 9158–9166.